Pergamon

Applied Geochemistry, Vol. 13, No. 8, pp. 921–939, 1998

PII: S0883-2927(98)00025-0
0883-2927/98 $ - see front matter

Geochemistry of natural and contaminated subsurface waters in fissured bed rocks of the Lake Karachai area, Southern Urals, Russia

Igor N. Solodov, Aleksandr V. Zotov, Aleksandr D. Khoteev, Aleksandr P. Mukhamet-Galeev, Boris R. Tagirov

Institute of Geology of Ore Deposits, Petrography, Mineralogy, and Geochemistry, Russian Academy of Sciences, Moscow, Russia

and

John A. Apps

Earth Science Division, Lawrence Berkeley National Laboratory, University of California

(*Received 22 May 1996; accepted in revised form 10 March 1998*)

Abstract—Hydrogeochemical investigations of natural and contaminated subsurface waters were conducted between 1992–94 in an area where liquid radioactive waste (RAW) was impounded in a small lake, and subsequently leaked into an underlying water bearing horizon. The waste was discharged from the radiochemical plant of the Mayak Amalgamated Industry near Chelyabinsk, Russia. The underlying water-bearing horizon in fissured metavolcanic rocks was penetrated by uncased observation wells in order to log the hydrogeochemistry. Logging was carried out using a specially designed hydrogeochemical probe, which contained 8 channels to measure continuously the temperature, pressure, electric conductivity, pH, Eh, the dissolved O_2 concentration, and the activities of Na, and NO_3 in the wells. The logging technique enabled the natural hydrogeochemical setting to be characterized and permitted delineation of bodies of contaminated waters of different origins using measurements of pH, pNa and pNO_3. The technique also permitted an evaluation of variations in the chemical composition of the RAW solutions due to radiolytic processes and to chemical interactions with the geologic medium. A conceptual model is proposed for the chemical evolution of the migrating contaminated subsurface waters in the area investigated.

INTRODUCTION

Radiochemical processing plants of the Mayak Amalgamated Industry (MAI) are located on the eastern slope of the Urals near the city of Chelyabinsk, Russia. MAI activities between 1948 and the present led to the construction of several reservoirs to contain low and intermediate level liquid radioactive wastes (RAW). The natural basins of the local Kyzyltash, Tatysh, and Karachai lakes and artificial reservoirs on the Techa River (Reservoirs 3, 4, 10, and 11), as well as the artificial Reservoir 17 were used to impound the liquid RAW (Fig. 1). Of these reservoirs, the greatest threat to the environment is presented by Lake Karachai (Reservoir 9) into which was discharged intermediate level NO_3-rich liquid RAW, containing 120 MCi of fission product radionuclides. The contaminated waters from this lake are infiltrating the groundwater system. The resulting plume of contaminated water follows the regional natural flow of the subsurface waters, migrating in both southerly and northerly directions from the lake (Fig. 2). The southern limb of the plume, containing about 60–70% of the contamination draining from the lake, poses a serious threat, because it is migrating towards the intake wells for the domestic drinking water supply for Novogornyi City.

Observations to determine the distribution of contaminated waters in the water-bearing horizon are carried out through a system of observation wells (Fig. 3). They are designed so that friable sediments and unstable fractured rocks in the uppermost section are isolated using cemented steel casings to a depth of between 5 and 15 m. On rare occasions the casing extends to a depth of 45 m. The underlying stable fractured rocks are penetrated without casing to a depth of between 50 and 120 m and in one well to a depth of 400 m. The completed internal diameter of the wells varies between 76–93 mm. Until 1992, groundwater hydrogeochemical observations in the wells were conducted primarily with a Simonov flow sampler [Maksimov, 1967]. Samples were collected, as a rule, from 3 intervals: 15–25, 40–50, and 80–100 m [Samsonova and Drozhko, 1996]. This sampling method suffers from the disadvantage that the most contaminated intervals of the subsurface water flow

are not clearly delineated, because of the inherent effect of compositional averaging over such broad sampling intervals.

To improve the sophistication and reliability of hydrogeochemical investigations, members of the Radiogeoecology Department, Institute of Geology of Ore Deposits, Petrography, Mineralogy, and Geochemistry, Russian Academy of Sciences, Moscow, Russia (IGEM), and the Scientific-Industrial Center (PALS), designed and fabricated an 8 channel hydrogeochemical probe (HGCP) for *in situ* measurement of T, P, E, pH, Eh, and O_2 concentration, and the activities of Na, and NO_3 (Plate 1). Such a probe is possible thanks to a method of pressure relief for standard potentiometric electrodes developed by Ben-Yaakov and Kaplan [1968], the integration of sensors and electrodes with an electric signal amplifier in the probe [Zotov *et al.*, 1981], and numerous independent confirmatory potential measurements in wells [Bottomley *et al.*, 1984; Solodov *et al.*, 1993], which has demonstrated the effectiveness of this method for the *in situ* study of subsurface waters.

TECHNOLOGY OF HYDROGEOCHEMICAL INVESTIGATIONS

The behavior of radioactive isotopes and dissolved stable substances in hydrogeochemical systems depends on the Eh–pH conditions and on concentrations of major complex-forming anions. Therefore, a determination of the existing physicochemical setting in the water-bearing horizon is of paramount importance.

Between 1992 and 1994, hydrogeochemical logging (HGCL) of uncased observation wells, in combination with interval sampling of subsurface waters by a non-hermetic flow sampler, was used for hydrogeochemical investigations in the vicinity of Lake Karachai. The choice of sampling intervals was based on logging results. The HGCL of observation wells was carried out with a standard mobile logging unit and automatic measurement system. The system includes the HGCP, an electronic data logger, a tachometric depth meter, and a portable PC AT386. The system allows for discrete and/or continuous logging of wells with automatic recording of depth and other parameters. The HGCP is equipped with 8 sensors for high precision resistivimetry, conductivimetry, amperometry, and potentiometry (Table 1), and precision measurements of T (Cu electrode resistivity), P (pressure transducer "silicon on sapphire"), E (sensor—4 conductive electrode measuring cell), O_2 (Clarke sensor), pH (glass electrode), Eh (Pt electrode), pNa (Na glass electrode) and NO_3 (liquid membrane electrode).

During logging, the sensors are interrogated every 2 sec, or more frequently, depending on the rate of probe penetration or withdrawal, and information is entered in digital form into the computer for every 10–50 cm interval throughout the depth of the well. The time required to log a well 200 m deep is no more than 30–45 min. The operation and reliability of the automatic measuring system was tested in the laboratory with equipment simulating field conditions, and in the field in conjunction with the conventional interval sampling method. The reliability of the system operation was confirmed by stable and repeatable measurements in wells. The precision and sensitivity of the system met specifications (Table 1). The *in situ* readings of the potentiometric sensors were in good agreement (10–15%) with results using other laboratory analytical methods. The stability of the system in operation was evaluated under natural physico-chemical conditions of the water-bearing horizon through a combination of continuous and discrete logging. With the sole exception of Eh measurements, the responses of the electronic circuits, communication lines, and electrochemical electrodes for all data channels were within the two-second interrogation time of the system (Fig. 4). During Eh measurements deviations and a sensor response lag were

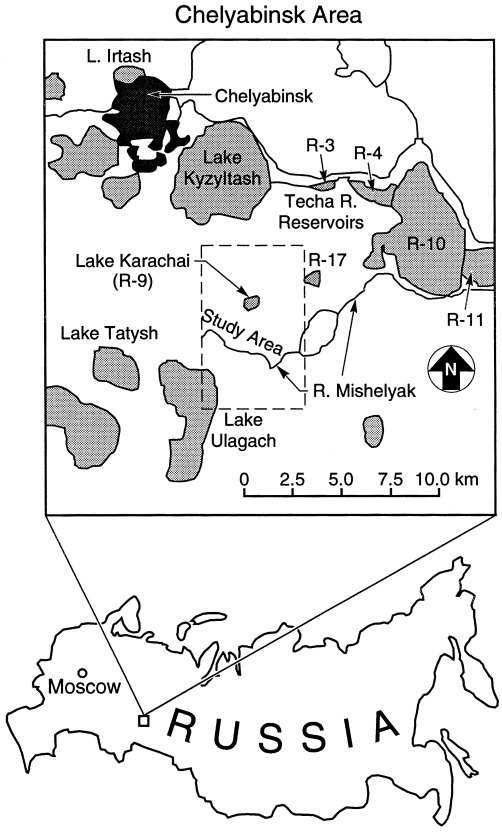

Fig. 1. Distribution of lakes and reservoirs at the Mayak site (from the work by Drozhko *et al.*, 1993). The area where detailed hydrogeochemical investigations were conducted, represented in Figs 2 and 3, is delineated by a dashed line.

Plate 1. Hydrogeochemical probe and associated data-logging equipment.

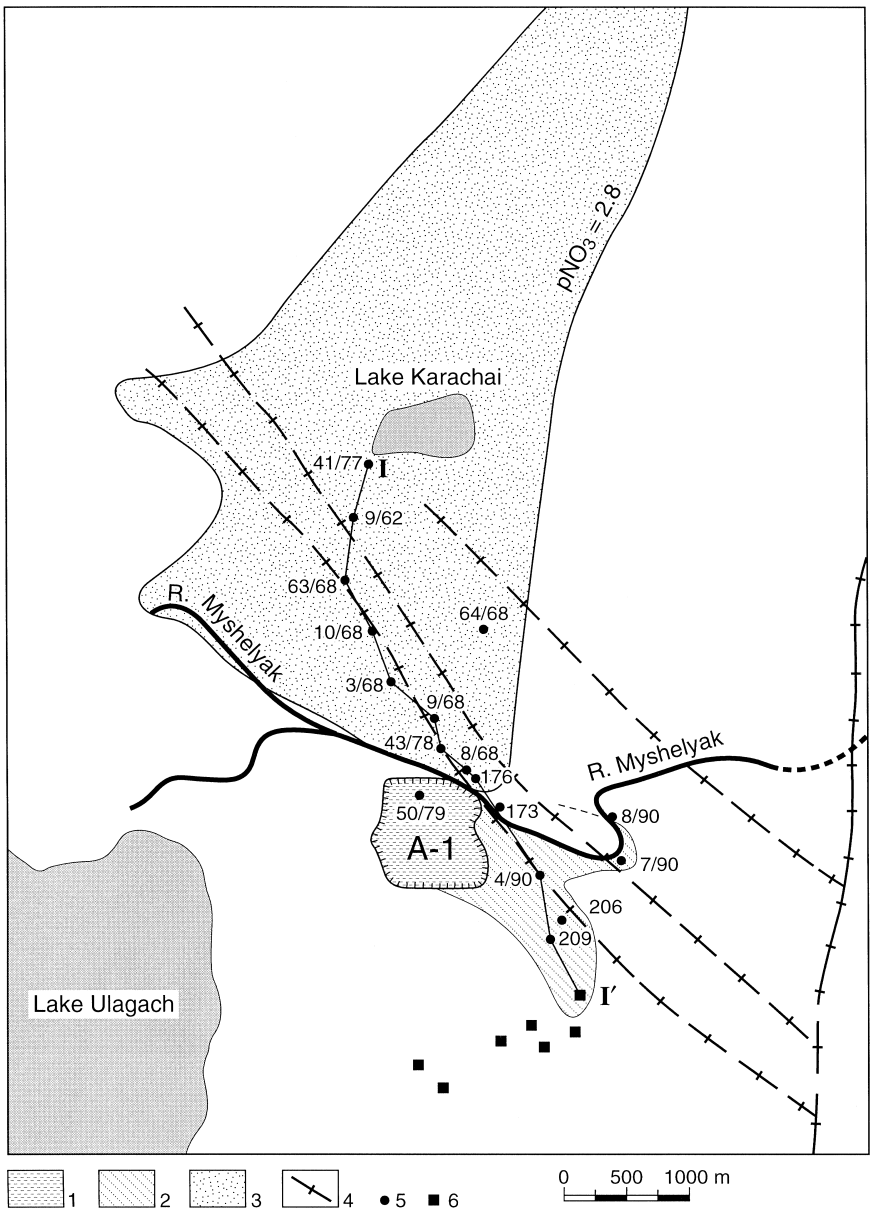

Fig. 2. Areal extent of contamination by liquid RAW from Lake Karachai and alkaline waters from the fly-ash impoundment of the Argayashskaya thermal power plant. 1—Old fly-ash impoundment (A-1) of the Argayashskaya thermal power plant and its associated plume, 2, of alkaline NO_3-bearing waters; 3—Plume of $NaNO_3$ brines from Lake Karachai; 4—Zones of schistosity and fracturing, and positions of assumed faults; 5—water sampling well; 6—water intake well. I-I′—line of geologic and/or hydrochemical cross sections.

observed, which was associated with the lack of inverse potential-charging in some areas of natural water distribution and with considerable physicochemical disequilibrium in the water solution–rock system due in part to the presence of the infiltrating liquid RAW.

Along with errors associated with the measuring system, hydrogeochemical logging can also be influenced by processes occurring within the well itself, which are not representative of those in the adjacent fractured bedrock. Firstly, there is a well known focusing effect on the fluid flow by uncased wells [Grinbaum, 1965]. Secondly, there is a distortion of the real distribution of parameters with well depth due to convective mixing of fluids with variable density in the well bore. In deep wells the latter effect results in the mixing of dense contaminated waters, with groundwaters, and an equalization of the concentrations of dissolved chemical components in the well bore. In order to determine the actual concentrations and distribution of the contaminated subsurface waters, such wells are flushed

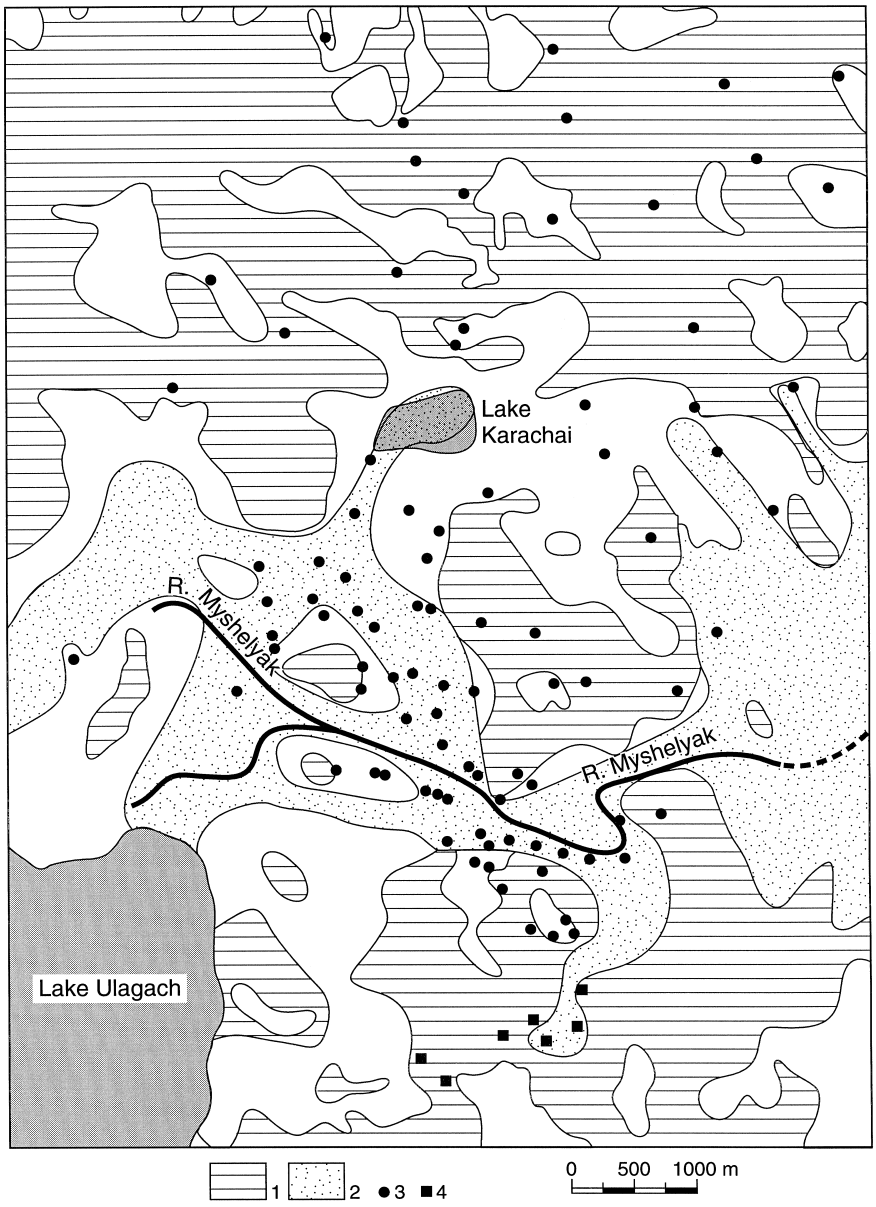

Fig. 3. Location of observation wells and hydrogeochemical zoning of subsurface waters in the vicinity of Lake Karachai. (Prepared by I.N. Solodov, 1994). 1—Hydrogeochemical subzone (SZ-1) of intensive vertical and lateral infiltration of O_2 bearing slightly acidic and almost neutral waters; 2—Hydrogeochemical subzone (SZ-2) of slow predominantly lateral migration of slightly-oxygenated and anoxic slightly alkaline waters; 3—Observation wells of the MAI Ecological Department; 4—Water intake wells.

with lake water 1–2 days before HGCL [Solodov *et al.*, 1994].

When interval sampling with the flow sampler, the subsurface water samples were transferred to plastic containers without exposure to the air and the containers sealed with rubber stoppers to prevent spontaneous degassing. The water samples collected in 1993 were analyzed using the following methods: potentiometry—Na, NO_3, NH_4, F; volumetric titrimetry—titrimetric alkalinity (as HCO_3), Cl, Ca, Mg; colorimetry—SO_4, Si, NO_2, P; flame photometry—K, Na; atomic absorption—Na, K, Cs, Ca, Mg, Sr, Ba, Fe, Mn; ion chromatography—acetate, oxalate, Cl, F, NO_3, NO_2, SO_4. Some of the above mentioned components and all others, presented in the following tables, were also determined using instrumental neutron-activation and quantitative spectro-chemical analysis. Total CO_2 was determined by Telesheva's method [Telesheva, 1964]. During sampling, any precipitates were dissolved in HCl and analyzed separately by the same methods. Analyses of the components present in the

Table 1. Parameters measured by the information-acquisition system during hydrogeochemical logging of observation wells

Parameter	Unit	Range	Error
T	° C	0–60	0.01
E	Sm/m	0.02–5	0.005
P	MPa	0–15	0.15%
pH	–log mol/kg	0–12	0.05
Eh, pNO_3, pNa	mV	–500–1800	10
Dissolved oxygen	mg/L	0–20	0.3
	Probe		
Length	mm	980	
Diameter	mm	65	
Mass	kg	5	

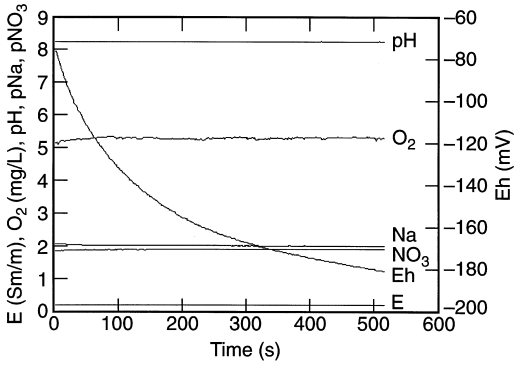

Fig. 4. Response time of O_2 and E sensors, and pH, pNa, pNO_3, Eh potentiometric electrodes during continuous and discrete logging in Well No. 176 at a depth of 181 m during October 1994. Parameters were monitored continuously at a specific depth immediately after inserting the probe into the well.

precipitates and in the aqueous phase are given in Tables 3 and 5. In order to evaluate the reliability of the Clark O_2 sensor readings of the HGCP, analyses of dissolved O_2 content in water samples were also carried out using Winkler's method immediately after logging selected wells.

Hydrogeochemical data were processed using the computer program, EQ3/6, Version 7 [Wolery *et al.*, 1992a,b], which employs the equilibrium constant method. Dissociation constants and solubility products of species in the aqueous solution and solid phases, respectively, used in the calculations, were taken primarily from Robie *et al.* [1979], Wagman *et al.* [1982], Reardon [1983], Johnson *et al.* [1991] and Grenthe *et al.* [1992] and corrected for temperature. Results are generally comparable to an earlier evaluation using the same analytical data, but conducted using the Gibbs free energy minimization method [Solodov *et al.*, 1993, 1994]. EQ3/6 calculates the true ionic strength of the solution, aqueous species activities and concentrations, Eh based on redox pairs, partial pressures of gaseous components, the percentage distributions of aqueous complexes of basis species and charge imbalance. The last procedure is carried out by comparison of molar amounts of positively and negatively charged species and is expressed as a percentage of the total charge. The saturation indices (SI) of minerals potentially associated with both natural and technogenic subsurface waters are also calculated. SI is defined as log(Q/K), where Q is the ion activity product and K is the solubility product of the mineral under consideration.

THE GEOCHEMISTRY OF NATURAL SUBSURFACE WATERS

Structure and composition of rocks hosting the shallow groundwater horizon

The structural setting of the region under study (Figs 2 and 3) is the core of the Gornenskaya syncline, a brachyform structure with gently dipping limbs. The syncline core is composed of Silurian and Devonian metavolcanic rocks of intermediate to basic composition. The metavolcanic rocks are irregularly faulted. The faults are identified mainly by linear schistose zones, which are located southeast of Lake Karachai (Fig. 2). The schistose zones form irregular lenses, which have been subjected to alteration in texture and mineral composition, and are broken into wide bands of sub-parallel fractures. A series of NW striking faults has been ident-

Table 2. Chemical Composition (in wt.%) of the Volcanic Bedrocks andComponent Minerals, [S. V.Yudintsev, personal communication]

Chemical Component	Whole Rock Analysis (40 samples)	Pyroxene	Amphibole	Epidote	Chlorite	Albite
SiO_2	50.96	50.48	54.78	39.68	32.43	68.16
TiO_2	0.84	0.67	0.96	0.11	0.05	0.06
Al_2O_3	15.35	2.79	1.87	23.11	21.19	19.44
Fe_2O_3	5.59	–	–	–	–	–
FeO	4.84	8.62	12.12	12.50	12.78	0.32
MnO	0.15	0.2	0.25	0.08	0.36	0.01
MgO	8.89	14.46	15.55	0.14	20.56	0.18
CaO	9.88	22.14	13.69	24.29	0.33	0.73
Na_2O	2.99	0.54	0.76	0.07	0.27	11.02
K_2O	0.51	0.0	0.02	0.02	0.03	0.08

Table 3. Chemical composition of natural (in subzones) and technogenic alkaline subsurface waters, associated with the fly ash impoundment, A-1, on the right bank of the Mishelyak River. Sampling and analysis conducted in September, 1992

Component	Measurement unit	SZ-1	SZ-2	Alkaline waters, (A-1)
pH_p	–	6.45	8.50	11.2
Eh_p (Pt)	mV	+400	+190	−185
SCO_2	mg/L	77	121	8.8
HCO_3		98	230	67.1
SO_4		26.9	115	38.4
Cl		7.1	53.2	36.7
SiO_2		17	15	5.4
NO_{3p}		1.5	6.2	28
NO_2		< 0.01	1.5	2.0
NH_4		< 1.8	< 1.8	< 1.8
Na		4.5	16	28
K		0.9	2.0	17.0
Ca		22	76	4
Mg		8.4	30	0.04
F	μ/L	300	300	300
Al		220	410	1200
Sr		210	290	120
Σ Fe		43.4	580	16.7
Mn		15.2	41	10
Ba		17	27	14
Zn		43	120	24
Pb		< 2	< 2	4.8
B		15	58	24
Ti		11	41	72
Cu		4.3	4.1	7.2
Mo		15	5.5	0.5
U		3.8	1.2	0.65
Ga		0	0	1.2
Ta		0	0	2.8
Total dissolved solids	mg/L	181	430	191

Notes: Subscript 'p' indicates *in situ* measurements in the water-bearing horizon.
Data on SZ-1 and SZ-2 each represent the averages of analyses from 5–8 wells.
The analysis of alkaline waters is represented by a sample drawn from Well No. 206.

Table 4. Saturation indices, SI, of various subzone waters in relation to potential mineral precipitates

Name	Composition	SZ-1	SZ-2	A-1
	Oxides and Hydroxides			
brucite	$Mg(OH)_2$	< −10.000	−3.747	−1.321
portlandite	$Ca(OH)_2$	< −10.000	< −10.000	−5.881
gibbsite$^+$	$Al(OH)_3$	**+2.609**	**+3.060**	**+0.845**
amorphous silica	SiO_2	−0.542	−0.607	−2.133
quartz	SiO_2	**+0.906**	**+0.842**	−0.684
schoepite	$UO_2(OH)_2 \cdot H_2O$	−3.344	−5.622	−6.014
	Carbonates			
magnesite	$MgCO_3$	−3.027	**−0.051**	−2.255
calcite	$CaCO_3$	−2.157	**+0.801**	**+0.319**
strontianite	$SrCO_3$	−2.131	**+0.433**	**+0.893**
witherite	$BaCO_3$	−0.449	**+2.194**	**+2.744**
gypsum	$CaSO_4 \cdot 2H_2O$	−2.548	−1.594	−3.182
celestite	$SrSO_4$	−3.755	−3.194	−3.841
barite	$BaSO_4$	**−0.353**	**+0.286**	**−0.270**
	Silicates			
*sepiolite	$Mg_4Si_6O_{15}(OH)_2 \cdot 6H_2O$	< −1.667	**+0.314**	**+0.405**
$\log P_{CO2}$		−1.844	−3.424	−8.054

Note: SI is defined as log(Q/K), where Q is the ion activity product and K is the solubility product. Those minerals that are near saturation or supersaturated are indicated by bold type.

*Normalized to one SiO_2

$^+$Gibbsite supersaturation is probably an artifact introduced by the analysis of total Al in solution containing colloidal particles.

ified within the southwestern schistose zone, discerned through variations in relief, thicker eluvium, and large He anomalies, i.e. 4.4×10^{-3} mL/L, where background values are normally in the range of 8.2 to 40×10^{-5} mL/L [Velichkin *et al.*, 1993]. In this area also, the metavolcanic rocks are much more intensively fractured.

The porosity within the metavolcanic rocks in regions between the large faults has been investigated to a depth of 80–100 m and is characterized by the following types of pores and fractures [Solodov *et al.*, 1994]: (1) voids in the form of plane-parallel microfractures and oriented linear pore-capillary systems from μm to tens of μm in size and with an effective porosity from 0.2–0.34%. In the depth interval from 80 to 1200 m, this effective porosity decreases and essentially vanishes in some sections, (2) hydraulically interrelated longitudinal and lateral systems of fractures formed as the result of visco-plastic and brittle deformation. The longitudinal fractures due to visco-plastic deformation are a few mm wide and between several cm and tens of cm long. Fractures due to brittle deformation are usually a few mm wide and rarely cm in width. Their length ranges between m and tens of meters.

In the upper part of the bedrock, to depths of several tens of m, voids are present due to the leaching of calcite from quartz-calcite and calcite stringers beneath the weathered and disintegrated crust, and also beneath modern river valleys and lake basins. This suggests the occurrence of deep circulating waters of surficial origin in permeable weathering zones.

In general, the fracture porosity and hydraulic conductivity in the bedrocks are as follows: in the upper part of the volcanic rock section to the depth of 20 m the porosity attains a maximum value of 2.8% and a hydraulic conductivity of 4–7 m/day; in the depth interval from 20 to 80 m, the values are 0.5–2.0% and 0.5–2.0 m/day, respectively; and below 80–100 m, they do not exceed 0.5% and about 0.2 m/day or less. Below 100 m, the voids diminish but do not entirely disappear. Intensely sheared schistose zones in the volcanic rocks were observed in holes up to 1200 m deep at the depths of 100–102 m, 515 m, and 832–843 m. These zones may serve as channels for deeply circulating contaminated waters.

The unweathered bedrocks are composed of metavolcanic rocks of andesitic to basaltic composition. An average chemical composition (based on 40 samples) is given in Table 2. The volcanic rocks have been subjected to regional metamorphism under greenschist facies conditions. The original rock forming minerals were represented primarily by pyroxene and plagioclase. Secondary minerals include amphibole, epidote, chlorite, albite and calcite. Carbonates are distributed irregularly in the rocks in concentrations ranging from 0.1–7.4 wt.% CO_2.

The mineral and chemical composition of volcanic rocks is considerably altered by weathering processes to a depth of 80–100 m. V.I. Myskin [cited in Solodov *et al.*, 1994] identified (from the bottom to the top) disintegration zones, zones of incipient clay alteration and clay alteration in the weathering zone profile. The maximum thickness of the uppermost clay alteration zone is 30 m. In the disintegration and incipient clay-alteration zones, various mixed layer minerals predominate among the secondary minerals. In the zone of incipient clay-alteration, the montmorillonite fraction increases, and vermiculite and kaolinite appear. In conformity with the distribution of clay minerals in the weathering profile, the sorption capacity of rocks increases progressively from the bottom to top.

Lake Karachai was originally an upland marsh. During the Pliocene–Quaternary epoch, thin, 0.1–0.2 m thick, peat and silt sediments accumulated in the marsh. The modern artificial lake area is, however, considerably larger than that of the pre-existing marsh, because the southern and western margins, composed of thin Late Miocene loams up to 2 m thick and in some places slightly altered exposed bedrock, have been flooded. The technogenic solutions infiltrate into the groundwaters through the altered rocks in the years of intensive precipitation when the lake level is elevated. The Mishelyak River valley to the S of Lake Karachai is filled with no more than 10–15 m of Late Miocene variegated clays. On the steep marginal slopes, the sedimentary cover is represented by loamy glacial deposits.

Processes affecting the chemical composition of natural subsurface waters

Lake Karachai and vicinity is a small region within the vast catchment area of the Tobol basin. In hydrodynamic terms, it is a zone of intensive water exchange. A N–S trending hydrogeological cross section I–I′, from Lake Karachai to the water intake wells for Novogornyi City (Fig. 2) shows that there is only one water-bearing horizon (Fig. 5), which consists of friable slightly permeable eluvial–glacial and thin alluvial sediments overlying relatively thick (80–100 m) fissured bedrocks. The groundwaters possess a normal hydrostatic gradient except in areas covered by clayey and loamy sediments where in years of heavy precipitation the groundwater head is slightly greater than the hydrostatic head.

The major recharge to the water-bearing horizon occurs as a result of precipitation. The magnitude of inflow into the fissured rock and variations in its chemical composition due to

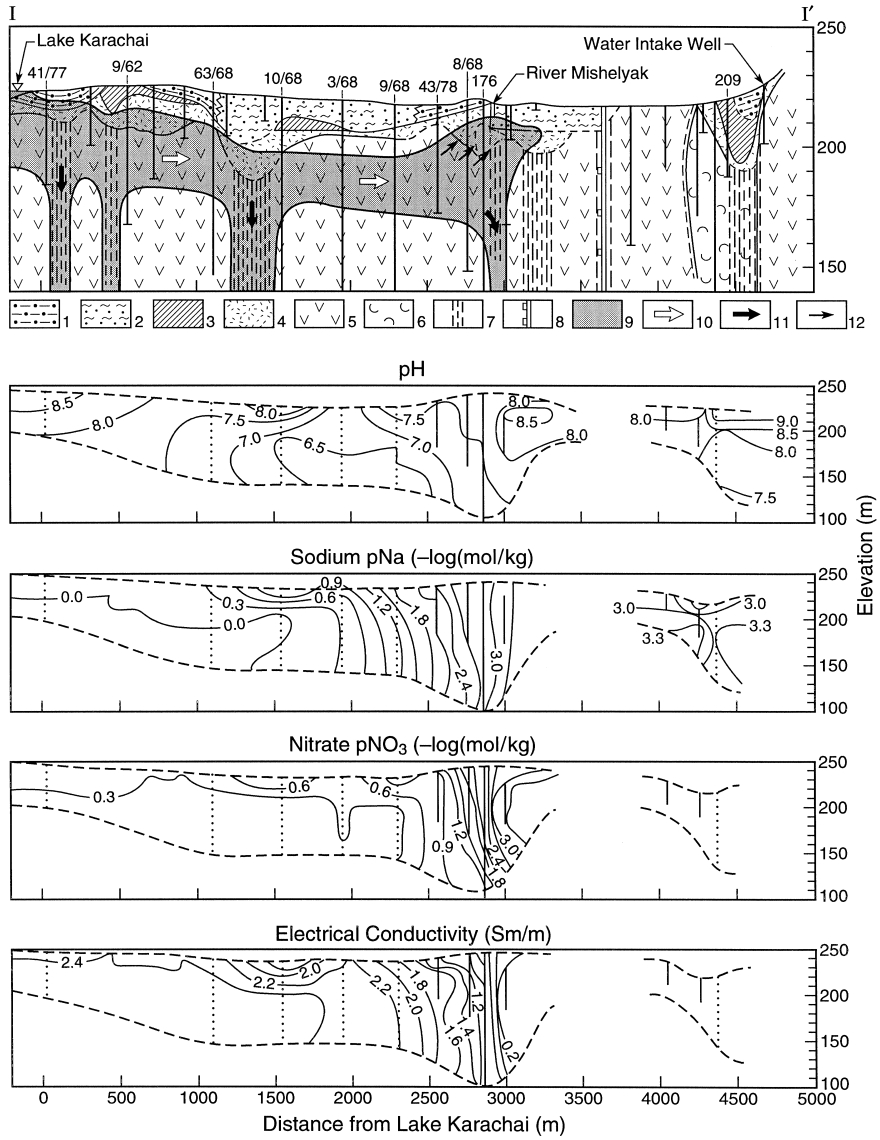

Fig. 5. Geologic cross section (prepared by B.T. Kochkin, 1993) and hydrogeochemical sections through the southern limb of the plume of contaminated water. The zone of open observation wells is delineated by a dashed line. Hydrogeochemical sections are prepared from hydrogeochemical logging results and interval sampling. 1—Late Miocene deluvial and proluvial loams with rare quartz pebbles; 2—Late Miocene alluvial sands and clays; 3—loams of the weathered crust; 4—weathered bedrocks; 5—porphyrites; 6—tuffs; 7—schistose zones; 8—a "rejuvenated" fault; 9—plume; 10—predominant direction of the contaminated water movement; 11—structural "traps" (zones of accumulation) of dense brines; 12—assumed direction of discharge of contaminated waters in the valley of the Mishelyak River.

reaction with the enclosing rocks depends directly on the local relief and the thickness of friable slightly permeable surficial sediments. An analysis of the HGCL results from observation wells situated beyond the influence of sources of contamination in combination with results of interval sampling of subsurface waters permits two hydrodynamic subzones to be distinguished, each with characteristic hydrogeochemical properties as described below:

Subzone of active vertical and lateral circulation of infiltrating waters (SZ-1). The SZ-1 subzone waters are distributed within elevated parts of the solid bedrock relief, where the fissured rocks outcrop or are covered by a thin layer of soil and loam (Fig. 3), and intense vertical and lateral circulation of surface waters occurs throughout the water-bearing horizon. Here, the base of the disintegration zone occurs at depths of no more than 40–60(?) m. The subzone is characterized by the

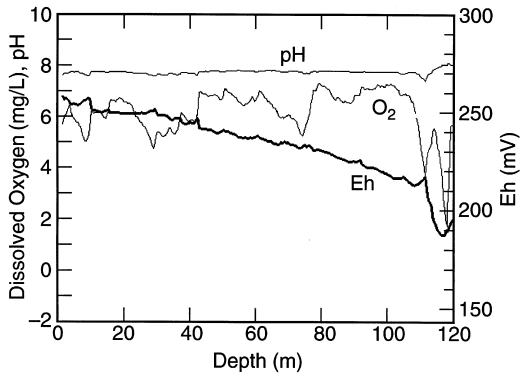

Fig. 6. Distribution of O_2, pH and Eh in subsurface waters of subzone SZ-1 on the left bank of the Mishelyak River, observed in Well No. 173 during October, 1994.

distribution of slightly acidic and near neutral (pH 6.4–7.4), oxidizing (Eh +200 to +480 mV), oxygen bearing (5–12 mg/L), and slightly mineralized (90–200 mg/L total dissolved solids) waters (Table 3, Fig. 6).

The SZ-1 subzone waters are chemically reactive in relation to the enclosing rocks, because they contain low concentrations of dissolved solids and their chemical composition has been modified only slightly through reaction with the enclosing rocks. As can be noted from Table 4, the water is unsaturated with respect to most carbonate and sulfate minerals. However, many smectite end member components, as well as illite and kaolinite remain supersaturated even after correcting for gibbsite supersaturation. Supersaturation with respect to these clay minerals is consistent with mineralogical observations of the secondary mineralogy of this shallow weathering zone, although uncertainties in the groundwater chemical analyses, clay mineral solid solution compositions and mineral thermodynamic properties limit further interpretation. The SZ-1 waters also contain elevated soil-derived concentrations of CO_2 in relation to surface waters. Thus, $\log P_{CO2}$ in the cited SZ-1 water is −1.84 (Table 4) compared with that in equilibrium with the atmosphere of −3.48.

Subzone of delayed lateral infiltration of groundwaters (SZ-2). Waters of the SZ-2 subzone are associated spatially with depressed areas of the solid bedrock relief, which are covered by slightly permeable alluvial, glacial and eluvial sediments (Fig. 3). Here the disintegration zone thickness varies from 80 to 100 m. Lateral groundwater migration, although less intensive than in the SZ-1 subzone, predominates in this subzone of the water-bearing horizon. The predominant groundwaters are slightly oxidizing with Eh varying between +70 and +160 mV in the lower part of the horizon. They are practically O_2-free (0–4 mg/L) and slightly alkaline where the pH ranges from 8.0 to 8.5 (Table 3). The total dissolved solid content (400–600 mg/L) of these waters increases as they

Table 5. Chemical composition of $NaNO_3/CO_3$ brines and subsurface waters in the lower part of the water bearing horizon (40–100 m below the surface) along the flow path from Lake Karachai to the Novogornenyi City water intake, September, 1993

Well No.	41/77	63/68	10/68	3/68	9/68	43/78	176	50/79	209
Distance, m	50	1100	1500	1900	2150	2210	2500	2800	4000
Depth, m	45	100	100	90	100	40	80	40	40
pH	8.05	7.33	6.6	6.45	5.85	7.39_p	7.33_p	8.42_p	8.12_p
NO_3 ,mg/L	45000	45000	52000	32000	27100	16690	3910	43	6.5
NO_2	4100	3600	6000	3800	4200	50	250	0.7	0.0
SCO_2	28800	10740	12200	11230	7080	490	93.6	134	41.8
HCO_3	4760	1220	1830	1160	952	266	251	220	120
CO_3	0	0	0	0	0	0	0	216	16.8
SO_4	360	400	350	165	287	384	200	111	42.2
Cl	120	90	105	80	88	49.7	162	54	46.9
CH_3COO	25	150	90	50	300	0.19	0.18	< 0.02	0.02
F	2	2	2	1.3	1.5	0.8	0.8	0.3	0.3
Humic acid	–	–	–	–	–	39.9	22.4	3.5	< 0.1
C_2O_4	0	0	0	0	1.76	0.016	0.009	< 0.001	< 0.001
SiO_2	2	6	6	16	16	25	21	21	2.5
Na	40000	24000	14000	11500	2200	337	46.3	42.5	35
K	310	260	140	130	60	6.9	5.1	1	1.7
^{137}Cs, Bq/L	< 300	< 300	< 300	< 300	< 300	< 4.5	< 4.5	< 4.5	< 4.5
Mg, mg/L	300	200	3900	4500	4100	1140	408	24	3.8
Ca	10	1400	9300	11300	10800	5300	720	66	1.6
Sr	210	260	250	250	180	28	12	0.31	0.29
NH_4	48	20	52	26	25	1.1	2.9	0.0	1.8
U	41	35	41	28	23	13	0.0037	0.0042	0.0017
Mn	< 1	< 1	80	90	60	–	–	–	–
TDS, g/L	110	83	95	72	54.5	24.3	5.83	0.514	0.173

Note: The components Ba, P, Fe, and Al are present in concentrations of less than 1 mg/L and are not included in the Table. A dash (–) means the absence of data. The subscript, p, indicates a field measurement.

approach equilibrium with the enclosing rocks. A thermodynamic analysis indicates that SZ-2 groundwater has attained saturation with respect to several carbonate components and barite (Table 4), and in common with SZ-1 waters, is supersaturated with respect to secondary clay minerals. $LogP_{CO2}$ is lower than in SZ-1 type water as a result of increased alkalinity. Note that the rather high degree of supersaturation with respect to calcite, where SI = + 0.801, could be attributed primarily to uncertainty in the pH measurement.

Within the fault zones and zones of increased fracturing, the SZ-2 subzone thickness increases to 80–120 m. In these parts of the water-bearing horizon, O_2-bearing (1–8 mg/L) oxidizing waters (Eh +110 to +210 mV) circulate. In one such well, No. 7/90, the O_2 concentration is observed to fall progressively from 8 mg/L at a depth of 20 m, immediately beneath the steel casing, to about 1 mg/L at a depth of 110 m. It is interesting to note that the dissolved O_2 content in the formation beneath the steel casing is unaffected by reaction with the steel casing in the upper sections of the wells where the steel corrodes through interaction with dissolved O_2, and forms H_2. In the steel casing interval, however, the Eh falls to −380 mV.

An analysis of background hydrogeochemical conditions suggests that an environment typical of subzone SZ-2 would have predominated between Lake Karachai and the Mishelyak River, prior to disposal of liquid RAW in the lake, i.e. in the area of the northern branch of the PaleoMishelyak river (whose axis coincides with the alignment of wells 41/77, 63/68, 9/68, and 8/68 in Fig. 2), slightly alkaline and slightly oxidizing waters would have been present. As will be shown below, technogenic geochemical processes have drastically changed this environment.

GEOCHEMISTRY OF CONTAMINATED SUBSURFACE WATERS

Liquid RAW was discharged into Lake Karachai for 43 years. At present it contains 120 MCi of beta-active radionuclides, of which 40% is ^{90}Sr and 60% is ^{137}Cs with concentrations of 3×10^{-3} and 9×10^{-3} Ci/L respectively. In the lake, 7% of the radionuclides are distributed in the water, 52% in silts, and 41% in loams at the bottom of the basin [Drozhko *et al*., 1993]. The volume of water in the lake is 0.2×10^6 m^3 covering an area of 0.1 km^2 with an average depth of 1.5 m. Since 1984, the lake has been largely filled with ferroconcrete blocks and rock from local quarries. The effluent discharged into the lake from the radiochemical plants consisted of radioactive slightly alkaline (pH 7.9–9.3) $NaNO_3$ brine. The dissolved salt load during the whole time the lake has acted as an effluent impoundment has varied between 16–145 g/L, and the brine density has proportionately varied between 1.006 and 1.095 g/cm^3. The major components of the dissolved salts were (in g/L): NO_3, 11–78; acetate (CH_3COO), 0.6–20; oxalate (C_2O_4), 0.9–14; SO_4, 0.12–1.3; and Na, 6–32. The concentration of secondary components was (in mg/L); Cl, 20–350; U, 13–196; Ca, 8–80; and Mg, 8–69 [Samsonova and Drozhko, 1996].

Lake Karachai straddles the divide between the Techa and Mishelyak river catchments. While acting as a liquid RAW impoundment, it accepted a volume of effluent 25 times greater than that of the basin. The dense effluent brine did not overflow the banks of the lake, but instead infiltrated the water-bearing horizon underlying the basin and displaced the natural subsurface waters. By 1993, a plume of $NaNO_3$ brine had displaced a preexisting volume of about 5×10^6 m^3 and covered an area of more than 15 km^2 in the water bearing horizon surrounding the lake. The mean velocity of the advancing NO_3 front at a depth of 60–100 m is presently estimated to be between 0.17 and 0.23 m/day [Glagolev and Samsonova, 1992]. By the time the present investigation had been concluded, the hydrogeochemical environments in the region between Lake Karachai and the Mishelyak River had been delimited, as is described further below (Table 5, Fig. 5).

In order to study the chemical behavior and interaction of the migrating plume with the preexisting groundwaters and aquifer rocks, waters were sampled from a series of wells along the traverse I–I′ and analyzed for their principal chemical constituents (Table 5). From these analyses, and HGCL, the nature and extent of the plume could be delimited within the aquifer. The $NaNO_3$ brine has completely displaced subsurface water near the lake. The brine chemical composition has also evolved with distance from the lake. Apart from dilution, precipitation, and hydraulic dispersion, the brine is modified under the influence of radiation due to radioactive decay and interaction with enclosing rocks. Thus, in the first well of the traverse, the brine has already evolved from a dominantly $NaNO_3$ composition to a $NaNO_3/HCO_3$ mixture. The predominance of molar concentrations of NO_3 over Na (e.g. see Fig. 7) also indicates processes involving the immobilization of Na by the weathered aquifer rocks. It is also clear that in the system under consideration, the various components differ in their capacity to migrate because of retardation or precipitation, and that NO_3 is least affected by these processes.

In the lake and immediate subsurface, the radioactive $NaNO_3$ brines are moderately alkaline with a pH 8–8.5. The alkalinity is due primarily to the radiolytic decomposition of acetate with the formation of HCO_3. The concentration of acetate was initially 0.6–20 g/L at the source, but decreases to

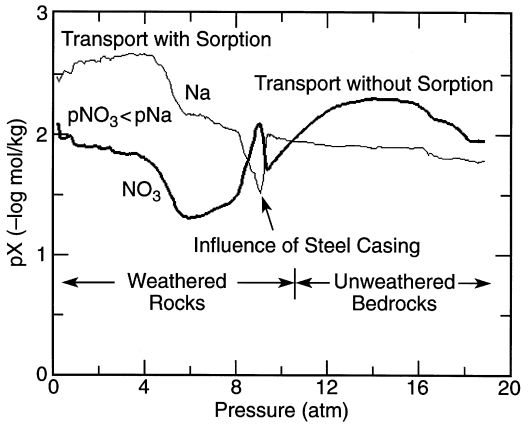

Fig. 7. Distribution of pNa, and pNO_3 as a function of hydraulic head in contaminated subsurface waters flowing from Lake Karachai as observed in Well No. 176 during October, 1994. The distribution reflects the differing migration capacity of Na in comparison with the conservative component, NO_3. Within the weathered rocks, Na is retarded in contrast to unweathered bed rocks, where retardation is minimal.

25–150 mg/L in the main body of the brine plume (Table 5). Radiolysis also appears to be associated with the destruction of oxalate in the system. However, it is probable that oxalate first precipitates as a low-solubility Ca oxalate precipitate, which then disintegrates by radiolysis. The relatively low concentration of Ca^{2+} and absence of oxalate in the brine, as observed in Well No. 41/77 (Table 5), could be attributed to this process. As a result of acetate and oxalate radiolysis, the total CO_2 concentration attains 28.8 g/L in Well No. 41/77, which is 360 times higher than in natural waters from a similar host rock environment.

After leaving the lake, the brine becomes progressively more acidic (pH ~ 6) and moderately oxidizing, e.g. the Eh is greater than +395 mV (Fig. 8). The increased acidity is due to the progressive precipitation of alkali–earth carbonates induced by the ion exchange of $2Na^+$ for Ca^{2+}, Mg^{2+} or Sr^{2+} in minerals of the geologic medium. In those regions of the water-bearing horizon in contact with the $NaNO_3/CO_3$ brine, Ca^{2+}, Mg^{2+} and Sr^{2+}

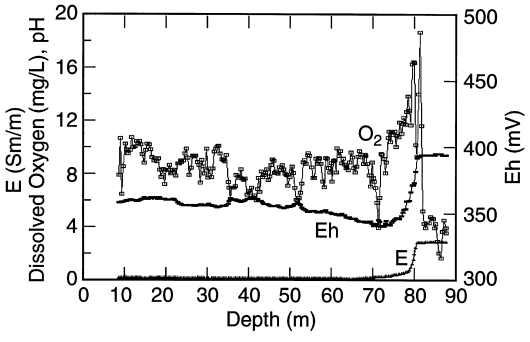

Fig. 8. Logs of E, Eh, and O_2 in Well No. 64/68 in 1994.

exchange most likely takes place in secondary clays, e.g. montmorillonite, in the clay alteration zones. However, Ca^{2+} removal from primary alumino-silicates, e.g. amphibole and epidote, and Mg^{2+} from amphibole and chlorite in deeper regions of the aquifer cannot be ruled out. The total concentrations of Ca^{2+} and Mg^{2+} exceed by tens to hundreds of times their concentrations in Lake Karachai. The Sr concentration in the brine samples is also 850 times more than in corresponding natural subsurface waters. The shift in pH also favors the formation of HCO_3, and an increase in the partial pressure of CO_2, which is confirmed by gas emanations consisting primarily of CO_2 from all wells located within a 1 km radius from the lake.

The change in oxidation state is explained by the partial radiolysis of the NO_3 in the brine to NO_2 (Table 5), correlating with data by Sharpaty and Proskurin [1962], and possibly to radiation or Na^+ induced dissolution or ion exchange, respectively, of metal cations, e.g. Fe^{2+} and Mn^{2+} that could also affect the redox state of the brine. Radiation of minerals leads to the distortion of atomic bonds and the formation of various defects in the crystal lattice, due to transfer of electrons from the valence zone to the conductance zone, and to other effects [Vovk, 1979]. These processes facilitate the transfer of chemical elements from minerals to the aqueous phase. Hydrated electrons, hydrogen, hydroxyl and hydroperoxide radicals, hydrogen peroxide, atomic, ionic, and molecular forms of hydrogen and oxygen [Allen, 1961] form during the disintegration of pure water when exposed to radiation. The products of water radiolysis accentuate many processes, some of which do not occur under natural conditions in the supergene zone [Vovk, 1979]. As a consequence, the alteration of feldspar into clay minerals, sulfides into sulfates and the oxidation of organic matter in the water and rocks is more intensive.

The oxidizing state of these waters may be explained by radiolysis in accordance with the concepts of Gutsalo [1972] and Vovk [1979], at least as reflected by the results of *in situ* measurements (Fig. 8). Dissolved O_2 with a concentration of 18 mg/L was observed at a distance of 1.3 km from the lake. Only an insignificant component (2–3 mg/L) of this dissolved O_2 is derived from the atmosphere. The balance has a radiogenic origin where, in the $NaNO_3/CO_3$brine, its concentration falls to 4 mg/L as the result of salting out (Fig. 8). The maximum concentration of O_2 is observed immediately above the brine plume and is 6 mg/L higher than the maximum dissolved concentration of O_2 (12 mg/L) in equilibrium with the atmosphere at the subsurface water temperature of 6°C. In this zone, at a depth of 80 m, the Eh is 65 mV higher than comparable shallow subsurface waters at 10 m depth. The slightly acidic condition and high oxidization state of such subsurface waters in the vicinity

Table 6. Distribution of aqueous species, expressed as mole percentages of the principal components, and other calculated parameters of $NaNO_3/CO_3$ solutions in the lower part of the water bearing horizon along the flow path from Lake Karachai to the Novogornyi City water intake

Well No.	41/77	63/68	10/68	3/68	9/68	43/78	176	50/79	209
Charge Imbalance, %	+22.2	+8.83	+16.8	+67.0	+50.9	+28.3	−9.96	+0.950	−45.30
True Ionic Strength, mol/kg	1.45	1.03	1.40	1.51	1.14	0.46	0.10	0.01	0.004
pH at 6°C	8.20	7.43	6.69	6.54	5.95	7.39	7.33	8.42	8.12
Eh,V. NO_2/NO_3	+0.40	+0.44	+0.47	+0.48	+0.51	+0.47	+0.44	+0.40	–
NH_4/NO_3	+0.33	+0.38	+0.43	+0.44	+0.48	+0.39	+0.39	–	+0.31
HAc/HCO_3	+0.20	+0.22	+0.27	+0.28	+0.29	+0.25	+0.24	+0.20	+0.21
ΣNO_3, mol/kg	1.03	0.799	1.02	1.17	0.793	0.344	0.0562	6.31E-4	1.05E-4
NO_3^-	99.87	98.2	90.5	88.9	86.7	89.6	96.9	99.5	100.0
$CaNO_3^+$	–	1.6	9.3	10.9	13.1	10.4	3.1	–	–
ΣNO_2, mol/kg	0.0900	0.0769	0.130	0.0844	0.0917	1.06E-3	5.47E-3	1.38E-5	–
NO_2^-	100.0	100.0	100.0	99.9	99.8	100.0	100.0	100.0	–
ΣHCO_3, mol/kg	0.661	0.240	0.276	0.261	0.162	0.0108	2.14E-3	2.27E-3	9.49E-4
$NaHCO_3(aq)$	52.4	41.1	19.0	15.4	2.0	0.9	–	–	0.5
HCO_3^-	44.4	51.7	40.9	37.9	25.9	62.5	77.7	94.8	96.7
$NaCO_3^-$	0.9	–	–	–	–	–	–	–	–
$MgHCO_3^+$	0.8	1.0	15.5	17.6	12.7	10.4	6.5	0.6	–
$CaCO_2(aq)$	–	–	–	–	–	1.0	–	0.9	–
$CaHCO_3^+$	–	2.2	10.8	12.1	10.0	18.0	5.9	1.1	–
CO_3^{2-}	0.7	–	–	–	–	–	–	0.9	–
$CO_2(aq)$	–	3.4	13.3	16.9	49.1	5.3	9.1	1.1	2.2
$UO_2(CO_3)_3^{4-}$	–	–	–	–	–	1.5	–	–	–
ΣNa, mol/kg	1.76	1.03	0.606	0.511	0.0961	0.0143	2.03E-3	1.62E-3	2.72E-3
Na^+	79.8	90.2	91.2	92.3	96.5	99.1	99.5	99.2	99.6
$NaHCO_3(aq)$	19.7	9.6	8.7	7.7	3.4	–	–		
ΣMg, mol/kg	0.0125	8.09E-3	0.160	0.189	0.169	0.0457	0.0169	8.98E-4	1.56E-4
Mg^{2+}	46.4	69.1	72.4	75.3	87.1	95.5	95.9	91.2	95.1
$MgHCO_3^+$	44.5	28.9	26.8	24.3	12.2	2.5	0.8	1.6	0.8
$MgCO_3(aq)$	8.6	1.0	–	–	–	–	–	–	–
$MgSO_4(aq)$	–	1.0	–	–	–	1.9	3.0	6.3	3.9
ΣCa, mol/kg	2.52E-4	0.0343	0.231	0.288	0.271	0.129	0.0181	1.50E-3	3.99E-5
Ca^{2+}	33.7	46.2	45.9	44.7	55.4	69.9	87.8	92.1	95.9
$CaNO_3^+$	33.1	37.5	40.8	44.2	38.4	27.7	9.60	–	–
$CaHCO_3^+$	24.5	15.1	12.9	10.9	6.0	1.5	–	1.6	0.8
$CaCO_3(aq)$	8.4	0.9	–	–	–	–	–	1.4	–
$CaSO_4(aq)$	–	–	–	–	–	–	1.9	4.7	2.9
ΣSr, mol/kg	2.42E-3	2.92E-3	2.84E-3	2.92E-3	2.06E-3	3.11E-4	1.38E-4	3.22E-6	3.31E-6
Sr^{2+}	43.9	49.1	47.6	45.1	53.4	65.0	84.6	93.6	96.3
$SrNO_3^+$	53.0	50.2	52.2	54.8	46.4	34.2	13.3	–	–
$SrCO_3(aq)$	2.8	–	–	–	–	–	–	–	–
$SrSO_4(aq)$	–	–	–	–	–	–	2.0	5.6	3.5
$\Sigma Ca/\Sigma Sr$	0.104	11.8	81.3	98.8	131.0	414.0	131.0	465.0	12.1

Note: species listed represent ≥99% of total concentration of given principal component.

Table 7. Variations in the saturation indices of potential mineral precipitates of $NaNO_3/CO_3$ brines and subsurface waters in the lower part of the water bearing horizon along the flow path from Lake Karachai to the Novogornyi City water intake

	Well No.	41/77	63/68	10/68	3/68	9/68	43/78	176	50/79	209
Mineral	Composition					SI				
Oxides and hydroxides										
brucite	$Mg(OH)_2$	−4.107	−5.640	−5.802	−6.014	−1.161	−4.739	−5.129	−4.033	−5.326
portlandite	$Ca(OH)_2$	< −10.000	< −10.000	< −10.000	< −10.000	< −10.000	< −10.000	< −10.000	< −10.000	< −10.000
amorphous silica	SiO_2	−1.696	−1.036	−1.001	−0.562	−0.567	−0.389	−0.449	−0.501	−1.379
quartz	SiO_2	**−0.247**	**+0.413**	**+0.447**	**+0.887**	**+0.881**	**+1.060**	**+0.999**	**+0.948**	**+0.069**
schoepite	$UO_2(OH)_2 \cdot H_2O$	< −10.000	−7.418	−6.698	−6.581	−4.759	−3.476	−4.355	−4.783	−3.882
Carbonates										
magnesite	$MgCO_3$	**+1.863**	**+0.718**	**+1.243**	**+1.125**	**+0.186**	**+0.391**	−0.510	**−0.336**	**−1.686**
lansfordite	$MgCO_3 \cdot 5H_2O$	**−0.292**	−1.394	−0.873	−0.993	−1.900	−1.662	−2.549	−2.372	−3.722
*huntite	$CaMg_3(CO_3)_4$	**+1.110**	**+0.540**	**+0.939**	**+0.819**	**−0.104**	**+0.186**	−3.784	−2.542	< −2.500
nesquehonite	$MgCO_3 \cdot 3H_2O$	−1.330	−2.449	−1.926	−2.046	−2.965	−2.740	−3.663	−3.457	−4.807
*disordered dolomite	$CaMg(CO_3)_2$	**+1.005**	**+1.248**	**+1.772**	**+1.400**	**+0.492**	**+0.868**	**−0.171**	**+0.138**	−1.617
calcite	$CaCO_3$	**+0.565**	**+1.718**	**+1.741**	**+1.614**	**+0.737**	**+1.284**	**+0.107**	**+0.552**	**+1.609**
aragonite	$CaCO_3$	**+0.419**	**+1.573**	**+1.596**	**+1.469**	**+0.591**	**+1.138**	**−0.039**	**+0.407**	−1.754
monohydrocalcite	$CaCO_3 \cdot H_2O$	**−0.251**	**+0.911**	**+0.933**	**+0.806**	**−0.066**	**+0.488**	−0.686	−0.240	−2.401
strontianite	$SrCO_3$	**+3.952**	**+2.975**	**+2.138**	**+1.913**	**+0.901**	**+0.959**	**+0.331**	**+0.272**	**−0.305**
rhodochrosite	$MnCO_3$	**< +1.097**	**< +0.534**	**+1.710**	**+1.551**	**+0.527**	–	–	–	–
rutherfordine	UO_2CO_3	< −10.000	−6.535	−5.127	−4.917	−2.892	−3.833	−5.226	−6.578	−5.731
Sulfates										
gypsum	$CaSO_4 \cdot 2H_2O$	−3.930	−1.483	−0.896	−1.163	−0.789	−0.537	−1.083	−1.721	−3.504
celestite	$SrSO_4$	−1.727	−1.428	−1.700	−2.064	−1.837	−2.087	−2.044	−3.233	−3.433
$\log P_{CO2}$		−1.174	−0.777	−0.090	+0.003	+0.218	−1.993	−2.501	−3.422	−3.479

Note: Values of SI in bold type indicate those minerals that are near saturation or supersaturated.
*Normalized to one CO_3.

of the lake favors the retention and migration of transuranic elements Am and Np [Hobart, 1990].

The distribution of some key geochemical parameters in a cross section of the plume along the I-I′ traverse is illustrated in Fig. 5. The bulk chemical compositions of technogenic brines from wells along the traverse (Table 5) were subjected to a thermodynamic analysis, and geochemically significant concentrations of migrating species of the major dissolved components between Lake Karachai and the Novogornyi City water intake, and saturation indices (SI) in relation to some potential secondary minerals were calculated and are summarized in Tables 6 and 7, respectively.

The thermodynamic analysis leads to several significant interim conclusions regarding the behavior of the liquid RAW in the subsurface environment. Before elaborating, however, several details concerning the thermodynamic analysis should be noted. Firstly, despite our acceptance of the pH measurements, those taken in the high ionic strength brines may be subject to uncertainties due to differences in the liquid junction potential across the fiber junction of the reference electrode in the brine when compared with the calibrating buffer solution. Secondly, the true ionic strength of the technogenic brines is greater than 0.5 mol/kg in 5 of the 9 analyses given, which exceeds the range normally recommended when using the extended form of the Debye–Huckel equation that was employed in the current analysis. However, uncertainties in the thermodynamic data used in the calculations are probably greater than the potential errors introduced by exceeding the recommended range of the electrolyte model. Secondly, the charge imbalance was corrected by adjustment of NO_3 concentration at 20°C for the first 5 analyses, and the species distribution and pH recalculated for ambient temperature (6°C). Adjustment of NO_3 concentration, does not have a major impact on the distribution of other species in the groundwaters or the calculated *in situ* pH, because it is weakly complexed. In the remaining analyses, the pH was measured in the field.

As noted above, the radiolytic decomposition of acetate and oxalate in the technogenic brines, leads to the formation of high concentrations of carbonate species in solution, while the high initial concentration of Na is progressively exchanged with alkali earth cations and results in increasing concentrations of Mg, Ca and Sr in the direction of plume movement. Table 7 shows that the brines are highly supersaturated with respect to calcite and several other carbonate minerals. Furthermore, the partial pressure of CO_2 in the brine approaches, and even exceeds one atmosphere as ion exchange of Na^+ progresses and secondary alkali–earth carbonates precipitate, driving down the pH. The identities of the carbonate minerals precipitating from solution within the plume are not known, but both field and laboratory evidence suggests that either low temperatures or high salinities, together with high levels of supersaturation, favor the formation of metastable carbonates (Fischbeck and Muller, 1971; Fischbeck, 1976: Davies *et al.*, 1977). Mg^{2+} in solution also retards calcite precipitation (Lippmann, 1973). However, the high transient level of supersaturation could induce rapid precipitation of fine particles with a substantial surface free energy contribution to the Gibbs free energy of the precipitating carbonates. Thus several factors will affect equilibration between carbonate precipitates and the technogenic plume. If the Ostwald's Rule of Stages [Ostwald, 1897] applies to the precipitation of carbonates within the plume, then according to Table 7, it is the least saturated of carbonate phases that are most likely to be precipitating, i.e. of those listed, monohydrocalcite and/or huntite, whose saturation indices are generally less than unity throughout the plume.

A recent experimental study concerning the kinetics of precipitation of carbonates from Ca–Mg chloride mixtures in solution at 25°C shows that both the rate of precipitation and the progressive evolution of successive phases is dependent on the aqueous Ca/(Ca + Mg) ratio [Babcan *et al.*, 1992]. Thus, while direct comparisons between the cited work and field conditions are not possible, it appears that the most likely precipitates at the prevailing Ca/(Ca + Mg) ratios would be either amorphous or finely crystalline Mg-calcite, or monohydrocalcite. Further investigations are warranted to clarify the kinetic and thermodynamic issues raised.

Radiolysis of the technogenic brine components leads to a state where the brine is not in internal equilibrium with respect to all redox pairs. However, it is noteworthy that the redox potentials defined by the N bearing redox pairs, NH_4/NO_3 and NO_2/NO_3, are reasonably consistent, although 200 mV higher than the HAc/HCO_3 redox pair (Table 6). Field measurements of Eh are consistent with the former, and with the high Mn concentrations observed in some of the analyzed samples (Table 5). At the measured pH of these solutions, the Eh must be of the order of +400 mV or less to ensure that Mn^{2+} remains in solution, probably in equilibrium with a rhodochrosite component of a precipitating carbonate solid solution. At higher Eh, Mn^{2+} would precipitate as Mn(III) or Mn(IV) oxides, and the concentration of Mn in solution would be far lower.

Of particular interest is the fate of ^{90}Sr during transport in the plume. As pointed out elsewhere in this paper, Sr^{2+} probably goes into solution, along with Mg^{2+} and Ca^{2+}, through ion exchange with $2Na^+$ in clay minerals, effectively diluting the ^{90}Sr concentration originally in the lake water by nearly

3 orders of magnitude. The Sr in aqueous solution is primarily in the form of the positively charged Sr^{2+} and $Sr(NO_3)^+$ species and possibly $SrHCO_3^+$ ($SrHCO_3^+$ was not incorporated in the EQ3/6 database used in the present study). However, Sr appears to be preferentially removed from solution through co-precipitation with Ca and Mg in amorphous or poorly crystalline carbonates, as the molal ratio of Ca/Sr shows a progressive increase from 0.10 to 412 between Well No. 41/77 and 43/78 in the plume with increasing distance from Lake Karachai (Table 6). Given that both Mg^{2+}, Ca^{2+} and Sr^{2+} ion exchange by $2Na^+$ and co-precipitation in carbonate occur concurrently as the plume advances, it would be expected that the ^{90}Sr radionuclide would be progressively diluted by nonradiogenic Sr, while being simultaneously immobilized in carbonate precipitates. The long term fate and state of immobilization of ^{90}Sr is contingent upon recrystallization of the carbonates, depletion of Ca in the ion exchange sites of clays, and the evolving composition of the infiltrating liquid RAW from Lake Karachai. Further study is merited.

Some comments on the behavior of U transport in the plume are also justified. Under the prevailing Eh–pH conditions in the plume, and in the presence of high concentrations of carbonate species, U sorption by rocks is improbable, because it is present in the form of negatively charged uranyl-carbonate complexes. Uranium solubility might be controlled by the precipitation of uranyl phosphates, but information on the concentration of PO_4^{3-} in solution would be required to test this hypothesis. At the leading edge of the plume, however, in Well No. 43/78, soddyite ($(UO_2)_2$ (SiO_4):$2H_2O$) saturates. It is thus possible that U will be transported and precipitate where carbonate precipitation has exhausted the complexing carbonate ligand for UO_2^{2+} in solution. Throughout the plume, U remains extremely unsaturated with respect to the uranyl carbonate, rutherfordine.

North and S of the Mishelyak River Eh–pH patterns in groundwaters differ significantly. In the region between Lake Karachai and the river, oxidizing slightly acidic waters predominate, but between the river and the Novogornyi City water intake the natural groundwaters are slightly oxidizing (Eh 0–+200 mV) and slightly alkaline (pH 7.5–8.0). Groundwaters also occur in this region that are alkaline (pH 9–11.2) and reducing (Eh from −150 to −250 mV). The latter are distributed in the vicinity of the water intake and have leached from the adjacent fly-ash impoundment, A-1, of the Argoyashskaya thermal power plant (TPP), which is located on the eastern bank of Lake Ulagach, and has been in operation since 1953 (Fig. 2 and Table 3). The alkalinity of leachates from the fly-ash impoundments is due to the high content of alkali–earth element (Ca and Mg) oxides in the ash. These waters are chemically reactive with the enclosing rocks and occur in the upper part of the water-bearing horizon, associated with demineralization due to the precipitation of carbonates and silicates (and possibly hydroxides) of Ca and Mg (Table 4), and ion exchange of Ca^{2+} for Na^+. They are also slightly enriched with other elements leached from the ash, e.g. K(?), Al, B, and Ga [Tauson, 1986]. As may be noted from Table 4, A-1 water is slightly supersaturated with respect to calcite, and strongly supersaturated with respect to the minor alkali earth carbonates, strontianite and witherite, but is undersaturated with respect to magnesite. It is probable that Mg^{2+} activity is controlled by saturation with respect to hydrated Mg silicates or aluminosilicates. Noteworthy is the extremely low calculated partial pressure of CO_2, which is reflective of the strongly alkaline character of these fly-ash leachates.

The demineralization process leads to waters of lower density, which contributes to the localization of these alkaline waters in the uppermost part of the hydrologic section to depths of 30–50 m. These modified alkaline waters presently invade the water intake wells from overlying horizons, in contrast to the dense brines of Lake Karachai, which would eventually migrate into the water intake wells from below (Figs 2 and 6).

DISTRIBUTION AND MIGRATION OF THE CONTAMINATED SUBSURFACE WATERS

The migration of the $NaNO_3/CO_3$ waters in the plume is reflected by variations in its chemical composition. The spatial distribution of the southern limb of the plume is determined by the physical character of the host medium, i.e. the relief of the base of the disintegration zone of the volcanic rocks, by the general orientation of fold structures, by the orientation of tectonic zones of predominant fracturing, and by partial discharges of subsurface waters near the lake through withdrawal of water for domestic water supplies, and through natural discharges to the Mishelyak River.

To precisely evaluate the scale of contamination and determine the predominant directions of migration of the contaminated waters, prognostic evaluations are required. Especially important is a delineation of the boundary between contaminated waters migrating from Lake Karachai, and other contaminated and natural bodies of groundwater. Nitrate is a useful indicator for the distribution of contaminated waters in the water-bearing horizon, as there are, apart from the brines from Lake Karachai, other sources of NO_3 in the subsurface waters, including those from stack gases and from fly-ash of the Argoyashskaya TPP.

Anomalous slightly acidic (pH 6–6.5) waters may be associated with stack gas aerosols, which are transported into surficial water-bearing soil horizons. These waters contain increased amounts of the following components [Zaikov *et al.*, 1991]: SO_4—up to a few hundreds of mg/L, NO_3—up to and exceeding the maximum permitted concentration for drinking water (10 mg/L as N), NO_2 and NH_4—fractions of mg/L, rarely more than one mg/L. Water leaching from the ash from the Argoyashskaya TPP is also a source of NO_3 in the subsurface waters. Such anomalies are encountered sporadically in the region around Lake Karachai. They are more common in areas of less acidic rocks and in the water-bearing horizon and are typically found at a depth up to 20 m, but rarely as deep as 40 m.

Nitrate anomalies of different origins may be distinguished by evaluating results of pH-pNa-pNO_3 logging using as criteria the pH of the groundwaters, the location of the NO_3 anomaly in the water-bearing section, and the pNO_3/pNa ratio. According to these criteria, where NO_3 anomalies are derived from stack gas aerosols, the subsurface waters are slightly acidic with a pH 6–7, whereas subsurface waters containing NO_3 anomalies associated with fly ash impoundments are alkaline and usually occur in the upper parts of the water bearing horizon. They contain up to 60 mg/L NO_3, and the ratio of pNO_3/pNa is >1 (Fig. 9). In contrast, NO_3 anomalies associated with technogenic brines from Lake Karachai, and occurring in weathered rocks, have a ratio of pNO_3/pNa, which is <1 (Fig. 7). Taking these criteria into account, the 100 mg/L concentration contour for NO_3, expressed as $pNO_3 = -\log(aNO_3) = 2.79$, was selected to unambiguously delineate the boundary of $NaNO_3$/CO_3 brines derived from Lake Karachai, because it exceeds the anomalous concentration of NO_3 in groundwaters with other origins (Fig. 2).

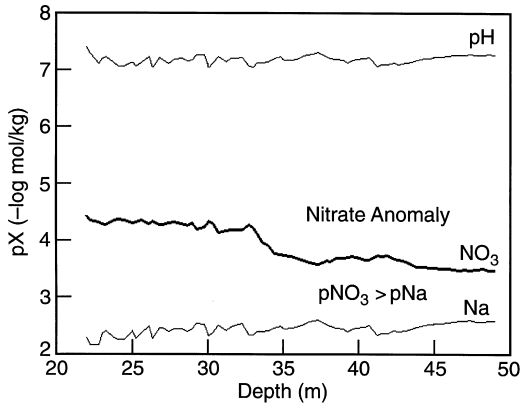

Fig. 9. Logs of pH, pNa and pNO_3 in Well No. 50/97 in 1994 showing the typical distribution of Na and NO_3 in the NO_3 anomalies associated with fly-ash impoundment A-1 of the Argayashskaya thermal power plant.

The distribution of non-conservative components in the plume, e.g. Na, U, ^{90}Sr, ^{137}Cs, ^{60}Co, which are retarded through reaction with the host rock can be compared with the migration of the "conservative" component, NO_3. Within the Mishelyak River and its flood plain, in the region where both the NO_3 solutions from the Lake Karachai and NO_3-bearing waters from the fly-ash impoundment are encountered (Fig. 2), anomalies of the mixed genesis have been observed lately.

Because of the density redistribution of solutions in observation wells that were not flushed before logging, it is impossible to establish precisely the distribution of flow in the vertical section of the water-bearing horizon. Hence, the lower limits of penetration of contaminated waters into the fissured volcanic bedrocks, often depicted in hydrogeological sections, e.g. Samsonova and Drozhko [1996], are probably inaccurate. Furthermore, the areal distribution of contaminated waters as determined using deep (mostly to 100–120 m) and shallow wells is also subject to substantial error. These limitations indicate that the actual distribution and migration of these waters and, correspondingly, the levels of contamination of subsurface waters, are presently known only imprecisely.

The groundwater migration pattern has been investigated mainly to the S of Lake Karachai (Fig. 2). An analysis of hydrogeochemical sections (Fig. 5) and resistivity observations in the wells flushed *a priori* with uncontaminated lake water [Solodov *et al.*, 1994], permit an important assumption to be made regarding the influence of rock fabric on the migration of the contaminated waters: a group of northwesterly striking faults and an associated zone of increased fracturing in conjunction with drainage by the Mishelyak River act as a hydraulic barrier to the movement of contaminated waters towards the Novogornyi City water intake. However, it is important to note that in the last 4 years, pNO_3 observed in wells on the left and right banks of the Mishelyak River has fallen. The change is evident in Well No. 8/90 where pNO_3 fell from 5 to 3 below 80 m depth between 1992 and 1993. Thus there are indications that insignificant amounts of contaminated waters of Lake Karachai provenance have been penetrating through this fault zone barrier to the right bank of the river, since 1993. Hydrodynamic processes affecting the migration of contaminated waters along their path from the lake to the river are presented in Fig. 5 in the form of a conceptual model (upper drawing).

CONCLUSIONS

Hydrogeochemical logging, used for the first time to study the chemical and radioactive contamination of subsurface waters in fissured volcanic

rocks in the vicinity of a surface impoundment the liquid RAW, indicates that this method is a reliable investigative tool for characterizing the geochemistry of natural and contaminated subsurface waters. Through such logging, it was possible to reconstruct the natural hydrogeochemical setting that existed in the water-bearing horizon prior to liquid RAW impoundment. The processes involving the chemical modification of natural groundwaters by infiltrating technogenic solutions were clearly identified. Among these processes, the most intensive are radiolysis of dissolved technogenic components acetate and oxalate with the formation of high concentrations of total CO_2 in solution, and the modification of Eh conditions through radiolysis of nitrate and the formation of considerable amounts of O_2, NO_2 and NH_4. The high initial concentration of technogenic Na^+ in solution induces ion exchange of Na^+ for Ca^{2+}, Mg^{2+} and Sr^{2+}, which in turn causes the precipitation of alkali metal carbonates and the selective precipitation of ^{90}Sr.

The application of pH-Eh-O_2 logging under natural conditions permits a quantitative evaluation of groundwater movement and the degree of hydrodynamic dispersion in the fissured bed rocks. Sodium-NO_3-pH logging in technogenic solutions permits the discrimination of NO_3 anomalies with different origins. Nitrate logging is a highly sensitive and detailed method for studying the distribution of contaminated waters, and may be recommended as the primary method of monitoring plumes of contaminated water emanating from sources similar to those investigated in this paper, particularly because practically all radiochemical recovery processes involve the use of nitrates, and the NO_3 ion is not significantly retarded in migrating groundwaters.

Hydrogeochemical logging also allows evaluation of gravitationally induced stratification of technogenic waters in fissured rocks and identification of zones of Na absorption from $NaNO_3/CO_3$ brines in structural traps, quantitative evaluation of hydraulic processes involving the dilution of technogenic brines through precipitation to a depth of 20–40 m, the hydrodynamic dispersion of the advancing front of the plume during migration through fissured rocks, and finally the determination and evaluation of ion-exchange and adsorption processes involving reaction of contaminants with the enclosing host rocks.

The immobilization of $NaNO_3/CO_3$ brines by structural traps may be a decisive factor in impeding the migration of contaminated waters through the water-bearing horizon. The existing factors involving the penetration of contaminated waters to depths exceeding 80–100 m within the $NaNO_3/CO_3$ brine plume (Fig. 5), suggest that structural traps of dense solutions could be employed as a natural means of storing highly mineralized radioactive solutions in the subsurface environment. It would, however, be necessary to determine their geometry and evaluate the sorbtive capacity and the degree of hydraulic isolation of these traps from surface waters.

Acknowledgements—We wish to express our gratitude to Academician N.P. Laverov, to Dr V.I. Velichkin of IGEM, to Dr E.G. Drozhko, Director of MAI and to Dr Chin-Fu Tsang, director of the Russian–American Center for Contaminant Transport Studies at the Lawrence Berkeley National Laboratory, California, USA (LBNL), for their cooperation and encouragement in completing this work and for critical discussions during the preparation of this paper for publication. We are also grateful to Mr H. Wollenberg (LBNL), who took part in the discussions concerning the publication of this paper, and who significantly improved its content, and also to Drs A. Simmons and E Sonnenthal (LBNL), Dr Y. Kharaka and anonymous external reviewers, who made valuable suggestions for improving the paper. The authors would also like to express their appreciation for the substantial assistance in the preparation of the paper and field work by Drs A.V. Zharikov and D.I. Krinov, members of IGEM, Russian Academy of Sciences, and by A.M. Tungusov, manager of the MAI Laboratories, and by analytical chemists, L.S. Shulik and Z.Yu. Kotova at IGEM for conducting the extensive chemical analyses of rock and water samples collected in the field. Finally, the authors would like to thank Ms L.J. Geniesse, LBNL, for drafting the figures. The preparation of this paper was supported in part by the Office of Energy Research, Office of Basic Energy Sciences (ER-BES) of the U.S. Department of Energy under Contract No. DE-AC03-765F00098.

Editorial handling:—Y. Kharaka

REFERENCES

Allen A. O. (1961) *The Radiation Chemistry of Water and Aqueous Solutions*. D. Van Nostrand Company, Inc., Princeton, New Jersey.

Babcan J., Iro S. and Sevc J. (1992) Experimental study of carbonate-formation kinetics in Ca^{2+}-Mg^{2+}-C_3^{2-} system at a temperature of 25°C. *Mineral. Slovac.* **24,** 1–7.

Ben-Yaakov S. and Kaplan I. R. (1968) High pressure pH sensor for oceanographic applications. *Rev. Sci. Instrum.* **39,** 1133–1138.

Bottomley D. J., Ross J. D. and Graham B. W. (1984) Borehole methodology for hydrogeochemical investigation in fractured rock. *Water Resour. Res.* **20,** 1277–1300.

Davies P. J., Bubela B. and Ferguson J. (1977) Simulation of carbonate diagenetic processes; formation of dolomite, huntite and monohydrocalcite by the reactions between nesquehonite and brine. *Chem. Geol.* **19,** 187–214.

Drozhko E. G., Sharalapov V. I., Posokhov A. K., Kuzina N. V. and Postovalova G. A. (1993) History, contamination and monitoring of water bodies at the P/A "Mayak". In *Proc. of 1993 International Conference on Nuclear Waste Management and Environmental Remediation. High Level Radioactive Waste and Spent Fuel Management*, (eds. P-E. Ahlstroem, C. C. Chapman, R. Kohout and J. Marek), 2, pp. 159–163. The American Society of Mechanical Engineers, New York.

Fischbeck R. (1976) Mineralogie und Geochemie carbonatischer Ablagerungen in europaeischen Hoehlen; ein

Beitrag zur Bildung und Diagenese von Speleothemen. *Neues Jahrb. Mineral., Abh.* **126,** 269–291.

Fischbeck R. and Mueller G. (1971) Monohydrocalcite, hydromagnesite, nesquehonite, dolomite, aragonite, and calcite in speleothems of the Fraenkische Schweiz, Western Germany. *Contrib. Mineral. Petrol.–Beitr. Mineral. Petrol.* **33,** 87–92.

Grinbaum I. I. (1965) *Geofizicheskiye Metody Opredeleniye Fil'tratsionnykh Svoystv Gornykh Porod (Geophysical Methods of Determining the Filtration Properties of Rocks)*. Moscow, Izdatel'stvo "Nedra" (in Russian).

Glagolev A. V. and Samsonova L. M. (1992) Method telefotometrii Skvazhin i ego ispol'zovanie dlya otsenki gidrogeologicheskikh parametrov vodonosnykh gorizontov (Method of well telephotometry and its application to the evaluation of hydrogeological parameters of water-bearing horizons.). Report of Scientific Investigations, Agreement with Mayak IA OH-92-05, Funds of Expedition N30 of SGE "Gidrospetsgeologiya", Moscow (in Russian).

Grenthe I., Konings R. J. M., Lemire R. J., Muller A. B., Nguyen-Trung C. and Wanner H. (1992) *Chemical Thermodynamics of Uranium*, (eds. H. Wanner and I. Forest). Nuclear Energy Agency, OECD. Elsevier Science Pub. Co..

Gutsalo D. K. (1972) Radiolysis of water as the source of free oxygen in the underground hydrosphere. *Geochem. Int.* **42,** 897–903.

Hobart D. E. (1990) Actinides in the environment. *Proc. Robert A. Welch Found. Conf. Chem. Res.* **34,** 378–436.

Johnson J. W., Oelkers E. H. and Helgeson H. C. (1991) SUPCRT92: A software package for calculating the standard molal thermodynamic properties of minerals, gases, aqueous species and reactions from 1 to 5000 bars and 0 to 1000°C. Laboratory of Theoretical Geochemistry, Univ. of California, Berkeley, California.

Lippmann F. (1973) *Sedimentary Carbonate Minerals*. Springer Verlag, Berlin.

Maksimov V. M. (1967) Spravochnoe Rukovodstvo Gidrogeologa (Reference Handbook of the Hydrogeologist), Leningrad: Nedra **2,** (in Russian)..

Ostwald W. (1897) Studien über die Bildung und Umwandlung fester Körper. *Zeits. Phys. Chem.* **22,** 289–330.

Reardon E. J. (1983) Determination of $SrSO_4$ ion pair formation using conductimetric and ion exchange techniques. *Geochim. Cosmochim. Acta* **47,** 1917–1922.

Robie R. A., Hemingway B. S. and Fisher J. R. (1979) *Thermodynamic properties of minerals and related substances at 298.15 K and 1 bar (10^5 Pascals) pressure and at higher temperatures*. U.S. Geol. Surv. Bull. 1452, reprinted with corrections 1979.

Samsonova L. M. and Drozhko E. G. (1996) Migration of high-density industrial waste solutions through fresh groundwaters. In *Deep Injection Disposal of Hazardous and Industrial Waste: Scientific and Engineering Aspects*, (eds. J. A. Apps and C-F. Tsang), Chap. 41, pp. 669–680. Academic Press.

Sharpaty V. A. and Proskurin M. A. (1962) O Promezhutochnykh Produktakh Radiliza Vody (About intermediate products of the water radiolysis). *In Tr. Vses. Sovescsh. po Radiatsionnoi Khimii, Moscow* **,** 122–126 (in Russian).

Solodov I. N., Kireev A. M., Zelenova O. I. and Umrikhin V. A. (1993) Technogenic oxidative changes in reduced uranium-bearing marine sandstone formations. *Litol. Polezn. Iskop.* **No. 6,** 84–96 (in Russian).

Solodov I. N., Velichkin V. I., Zotov AV , Kochkin B. T., Drozhko E. G., Glagolev A. V. and Skokov A. N. (1994) *Distribution and Geochemistry of Contaminated Subsurface Waters in Fissured Volcanogenic Bed Rocks of the Lake Karachai Area, Chelyabinsk, Southern Urals*, Russian-American Center for Contaminant Transport Studies. Lawrence Berkeley Laboratory. Rept. LBL-36780 (UC-603).

Tauson L. V. (1986) Problems of geochemistry of technogenesis. *In Collected Works Geokhimiya Tekhnogeneza (Geochemistry of Technogenesis), Geokhimiya Tekhnogeneza, Novosibirsk* **,** 3–9 (in Russian).

Telesheva R. L. (1964) Opredelenie Uglekisloty Polumikrometodom v Izvestnyakakh, Dolomitakh, Magnezitakh, Sideritakh i Drugikh Porodakh Soderzhashchikh Karbonaty (Determination of carbonic acid by submicromethod in limestones, dolomites, magnesites, siderites and other rocks with carbonates). In *Khimicheskii Analiz Mineralov i ikh Khimicheskii Sostav*, pp. 140–142. Moscow: Nedra, (in Russian).

Velichkin V. I., Solodov I. N. and Tarasov N. N. (1993) Otsenka Zashchitnykh Svoistv Geologicheskoi Sredy Raiona PO "Mayak" na Osnove Geologicheskikh, Gidrogeologicheskikh i Petrologicheskikh Issledovanii. (Evaluation of Protective Properties of the Geological Environment of the IA "Mayak" Area on the Basis of Geological, Hydrogeological, and Petrological Investigations). Report on Scientific Investigations (Second Stage). Moscow: OGR IGEM, Russian Academy of Sciences (in Russian).

Vovk I. F. (1979) Radioliz Podzemnykh Vod i ego Geokhimicheskaya Rol' (Radiolysis of Subsurface Waters and its Geochemical Role). *Moscow: Nedra* **231,** (in Russian).

Wagman D. D., Evans W. H., Parker V. B., Schumm R. H., Halow I., Bailey S. M., Churney K. L. and Nuttall R. L. (1982) The NBS tables of chemical thermodynamic properties, selected values for inorganic and C1 And C2 organic substances in SI units. *J. Phys. Chem. Reference Data* **11** (Suppl. 2), 392.

Wolery T. J. (1992) *EQ3/6, A software package for geochemical modeling of aqueous systems: package overview and installation guide*. Lawrence Livermore National Laboratory Report UCRL-MA-110662 PT I.

Wolery T. J. (1992) *EQ3NR, A computer program for geochemical aqueous speciation-solubility calculations: theoretical manual, user's guide, and related documentation*. Lawrence Livermore National Laboratory Report UCRL-MA-110662 PT III.

Zaikov G. E., Maslov S. A. and Rubailo V. L. (1991) *Kislotnye Dozhdi i Okruzhayushchaya Sreda (Acid Rains and the Environment)*. Khimiya, Moscow (in Russian).

Zotov A. V., Prikhod'ko V. A. and Sheimin E. G. (1981) pH-Eh-izmereniya termal'nykh vod v glubokikh skvazhinakh (Measurement of pH-Eh of thermal waters in deep wells). *Dokl. Akad. Nauk SSSR* **260,** 436–440 (in Russian).